

# Computational Investigation of the Effects of Leading-Edge Bluntness on Drag at Supersonic Speeds

M. Abhinav, V. Narasimha Reddy  
Department of Mechanical Engineering,  
Malla Reddy Engineering College,  
Secunderabad-500100, India

**Abstract-**The present paper discusses the computational investigation of the effects of leading edge bluntness on drag at supersonic speeds by using CFD software FLUENT at different supersonic Mach numbers. The main design factors that affect projectile configuration is the lift and drag force, with lowest drag as possible. In this study three widely known nose shapes with different geometries are considered.

The present paper would deal with the computation of the drag or various configurations considered with respect to the Mach number and bluntness or fineness ratios ( $n = 0.5$ ,  $n = 0.667$ ,  $n = 0.8$ ). As fineness ratio and Mach number increases the overall drag decreases. The drag is compared based on the 3 main drag components; skin friction drag, wave drag and base drag. For this paper only the conical nose shape with different fitness ratios are presented. The results from the flow analysis for various configurations have been analysed and presented in the report.

**Keywords-** Mach number; Fineness ratio; Drag force; Nose cone configurations; Flow velocity.

## I. INTRODUCTION

### A. Blunt Nose Cones

Supersonic vehicles are commonly designed and manufactured with blunt nose. Supersonic cruise vehicles need low drag to efficiently maintain velocity. Understanding, analyzing and predicting high speed flow around blunt bodies thus poses a practical and important engineering problem.

Gas flow around the fore body of blunt-nose vehicles is typically clean, and subjected to few upstream disturbances. The effect of nose cone geometry on penetration performance has been studied for decades. A variety of analytical methods have been performed to attempt to optimize the nose shape for a penetrator. The new shape design was created by diving the nose shape into line segments and searching through numerical space for the combination of line segment slopes that produced the nose geometry with the lowest nose shape factor. This nose shape factor is derived using penetration mechanics theory. The new design should provide an updated perspective on nose shape design [1].

### B. Blunt Body Flows

The figure.1 shows the diagram of air flow around a cylinder at Mach 4, the initially uniform free-stream flow is processed by a detached bow shock (S), and subsequently enters the shock layer.

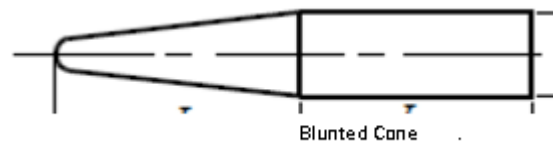


Fig. 1. Nose cones

The hypersonic free stream is undisturbed by the down-stream obstacle, since the speed of information propagation in that region is slower than the flow speed. The shock wave is strongest at the point where it is normal to the free stream inflow (N). Away from this location, the bow shock becomes oblique to the inflow and weakens, due to relief afforded by the body curvature.

Inside the shock layer, the sonic surface (L) demarks the transonic interface between subsonic and supersonic flow. For lower speed supersonic inflow, the interface would occur further downstream than pictured. Within the subsonic region bounded by the sonic surface, shock, and body, flow information is everywhere propagated in all directions via pressure waves. The stagnation point (T), is located within the subsonic region, and is defined as the location where flow impinges on the body in the surface-normal direction. In the case of an ideal, calorific ally perfect gas, and an adiabatic body surface, flow pressure and temperature are highest at the stagnation point. The viscous boundary layer (B) is initiated at the stagnation point, and grows along the body surface in the downstream direction. In the presence of adverse pressure gradients, particularly in the shadow region behind the body, the boundary layer may at some stage separate from the surface [2].

As gas advents out of the subsonic region, it expands (E) and accelerates into the in-creased volume between shock and body. The decreasing shock angle, combined with the effects of flow expansion, usually results in a decrease of both pressure and temperature. At points downstream of the subsonic region, the increased flow speed means that pressure waves cannot travel back upstream. Hence, the state of the downstream flow field does not affect the subsonic region, except possibly via electromagnetic field or the boundary layer. Hence, the simulation of a complete supersonic vehicle is not necessarily required to accurately reproduce the flow around its nose. Figure.2 shows a blunt body in a supersonic stream.

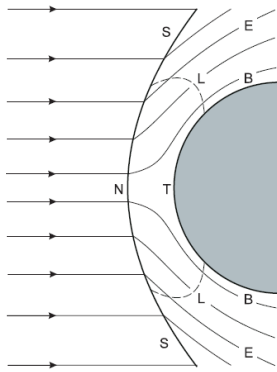


Fig. 2. A blunt body in a supersonic stream

**C. Nose Cone Shapes And Equations**

**i. General Dimensions**

In all the following nose cone shape equations, L is the overall length of the nose cone and R is the radius of the base of the nose cone. y is the radius at the point x, as x varies from 0, at the tip of the nose cone, to L. The equation define the 2-dimensional profile of the nose shape. The full body of revolution of the nose cone is formed by rotating the profile of the nose cone around the centerline (C/L).

The figure.3 shows the nose cone dimensions used in equations.

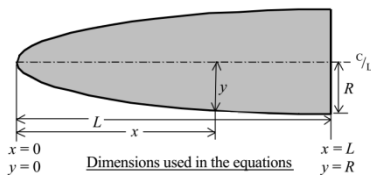


Fig. 3. General Nosecone Dimensions

**ii. Fineness Ratio**

Fineness ratio is a term used in naval architecture and aerospace engineering to describe the overall shape of a streamlined body. Specifically, it is the ratio of the length of a body to its maximum width; shapes that are “short and fat” have low fineness ratio, those that are “long and skinny” have high fineness ratios. Aircraft that spend time at supersonic speeds generally have high fineness ratios, a canonical example being Concorde.

At speeds below critical mach, one of the primary forms of drag is skin friction. As the name implies, this is drag caused by the interaction of the airflow with the aircrafts skin. To minimize this drag, the aircraft should be designed to minimize the exposed skin area, or “wetted area”, which generally implies the fuselage should be somewhat “egg shaped”, with a fineness ratio about 4.5. A good example of such a design is the Questair Venture.

Most aircraft have fineness ratios significantly greater than this, however. This is often due to the competing need to place the tail control surfaces at the end of a longer moment arm to increase their effectiveness. Reducing the length of the fuselage would require larger controls, which would offset the drag savings from using the ideal fineness ratio. An example with of a high-performance design with an imperfect fineness ratio is the Lancair.

**D. Aerodynamics**

Aerodynamics is the branch of science that deals with the motion of air and the forces on bodies moving through the air. There are four forces that act on a rocket: weight, lift, drag, and thrust. Weight is a force that is always directed toward the centre of the Earth. To overcome the weight force, aircraft generate an opposing force called lift. Lift is generated by the motion of the aircraft through the air. Most of the lift is generated by the wings. In most rocket designs, fins are more engaged to steer or direct the airflow for flight stability, instead of providing lift. Drag is a force that opposes the upward movement of the rocket. It is generated by every part of the rocket. Drag is a sort of aerodynamic friction between the surface of the rocket and the air. To overcome drag, aircraft and rockets use a propulsion system to generate a force called thrust. In the present study we are dealing with the variation of the drag force over blunted nose cone profiles. So let us discuss about aerodynamic drag force in detail.

**II. COMPUTATIONAL REPRESENTATION**

The first objective of this study is to obtain the steady-flow field (inviscid flow) results for blunt-nosed profiles of various fineness ratios at Mach 2. The second objective is to obtain the simulations of viscous flow over blunt nose cone profiles of fineness ratios  $L/D = 0.5, 0.667, 0.8$  configuration at Mach 2, Mach 3 and Mach 4. This chapter describes the problem and the computational arrangements made to achieve these two objectives.

**A. Problem Description**

Blunt nose profile configurations. (Axisymmetric profiles)

- i. Fineness ratio  $L/D = 0.5$   
 Horizontal length  $x = 27.9$  mm  
 Vertical length  $y = 9.844$  mm  
 Diameter  $d = 20$  mm  
 Area  $A = 0.000183093$  m<sup>2</sup>

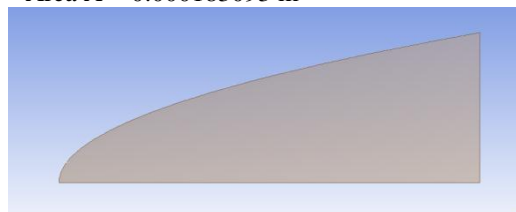


Fig. 4. Blunt-nosed profile of fineness ratio  $n=0.5$

Figure.4 shows a blunt-nosed profile of horizontal length 27.9 mm and vertical length of 9.844 mm and diameter of this profile is 20 mm area is 0.000183093 m<sup>2</sup>. Since this profile is studied in this computational study for the variation of coefficient of drag over it in supersonic flows under inviscid case at mach 2 and viscous case at mach 2, 3 & 4. Since it is axisymmetric profile only half of the profile is used for this study.

- ii. Fineness ratio  $L/D = 0.667$   
 Horizontal length  $x = 37.2$  mm  
 Vertical length  $y = 9.844$  mm  
 Diameter  $d = 20$  mm  
 Area  $A = 0.000219678$  m<sup>2</sup>

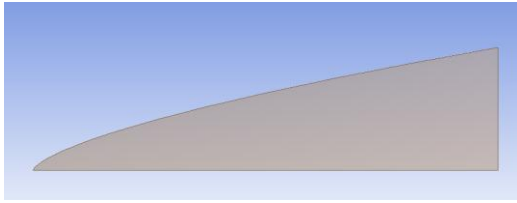


Fig. 5. Blunt-nosed profile of fineness ratio  $n = 0.667$

Figure.5 shows a blunt-nosed profile of horizontal length 37.2 mm and vertical length of 9.844 mm and diameter of this profile is 20 mm and area is 0.000219678 m<sup>2</sup>. Since this profile is studied in this computational study for the variation of coefficient of drag over it in supersonic flows under inviscid case at mach 2 and viscous case at mach 2, 3 & 4. Since it is axisymmetric profile only half of the profile is used for this study.

- iii. Fineness ratio  $n = 0.8$   
 Horizontal length  $x = 44.6$  mm  
 Vertical length  $y = 9.844$  mm  
 Diameter  $d = 20$  mm  
 Area  $A = 0.000243659$  m<sup>2</sup>

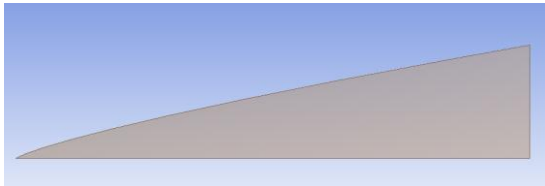


Fig. 6. Blunt-nosed profile of fineness ratio  $n = 0.8$

Figure.6 shows a blunt-nosed profile of horizontal length 44.6 mm and vertical length of 9.844 mm and diameter of this profile is 20 mm and area is 0.000243659 m<sup>2</sup>. Since this profile is studied in this computational study for the variation of coefficient of drag over it in supersonic flows under inviscid case at mach 2 and viscous case at mach 2, 3 & 4. Since it is axisymmetric profile only half of the profile is used for this study.

In this study we are performing the flow analysis over these profiles to know the variation of drag on them in supersonic flows at different mach numbers under different conditions.

### III. NUMERICAL ASSUMPTIONS

Several simplifying assumptions are made in the simulations. The models used in this investigation are assumed to be on a flat base. In view of the small scale of the flow field (i.e., the nose region), laminar flow is assumed. The free stream Reynolds number is roughly  $5.0 \times 10^7/m$ . The actual Reynolds number (per meter) is much smaller along the body surface inside the cavity and outside the cavity near the lip, because of the low-speed flow. The wall temperature is assumed isothermal ( $T_{wall} = 300$  K) and the flow is assumed calorically perfect considering the previous numerical studies. The models are axisymmetric. Figure.7 shows the flow domain assumed in the present investigation.

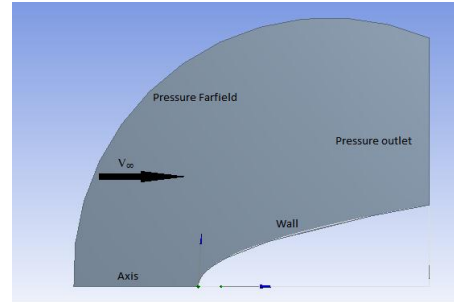


Fig. 7. Figure showing the flow domain

Boundary conditions for the assumed blunt nosed profiles are defined as follows

TABLE I. BOUNDARY CONDITIONS FOR ASSUMED BLUNT NOSE PROFILES

		$n = 0.5$	$n = 0.667$	$n = 0.8$
Pressure	farfield (Pascal)	101325	101325	101325
Temperature	(kelvin)	300	300	300
Mach no	Inviscid	2	2	2
	Viscous	2, 3, 4	2, 3, 4	2, 3, 4

These conditions are specified for every profile assumed to be in this investigation and the flow simulation is performed on these profiles.

### IV. FLOW ANALYSIS OVER BLUNT BODIES

Rapid technological advancements have increased computer power tremendously. With the boost of processor speed and graphic software, computers are widely used in aerodynamic prediction modelling. This led to a new field of study named computational fluid dynamics (CFD). CFD uses fundamental conservation laws, like Navier-Stokes equations, to numerically solve fluid flow over a region of interest with specific boundary conditions. It provides an excellent cost-effective tool to study fluid flows and complements empirical methods and wind tunnel testing.

In this study, the computer program ANSYS CFX was used to compute the axisymmetric flow over various conical blunt bodies which are defined. ANSYS CFX uses the full Navier-Stokes equations to solve. ANSYS CFX is an advanced CFD solver that has the facilitating technologies of geometry handling and meshing pre- and post-processing all housed within and integrated into the ANSYS Workbench. ANSYS Workbench has a platform's project page that can launch and track the geometry module, mesh module, setup pre-processor, solution module and results post-processor. These modules form the process of creating a CFD analysis on various conical blunt nose profiles.

**A. Assessment Of Conical Blunt Nose Profiles**

**i. Creating Geometries**

Ansys workbench was used to sketch and design a conical blunt nose with generated co-ordinates in the excel sheet with necessary calculations. Dimensions of the generated axisymmetric conical blunt nose profiles are as follows

TABLE II. GEOMETRIC CONDITIONS OF BLUNT NOSE PROFILES

Bluntness ratio	Boundary Horizontal length	Boundary Vertical length	Profile length (horizontal)	Profile length (vertical)
0.5	42.9	30	27.9	9.844
0.667	52.2	30	37.2	9.844
0.8	59.6	30	44.6	9.844

**ii. Meshing Geometries**

After creating the geometries in the Ansys workbench design modeller, that geometry files are opened in the mesh for meshing purpose. The meshing data for each profile is shown in the following table. Figure. 8 meshing of conical blunt nose profile.

TABLE III. MESHING OF BLUNT NOSE PROFILES

Bluntness ratio	Horizontal mesh	Vertical mesh	Profile mesh	bias
0.5	200	200	500	200
0.667	200	200	600	200
0.8	200	200	700	200

By following the above mentioned data conical blunt nose profiles are meshed. Final generated mesh files are shown as follows.

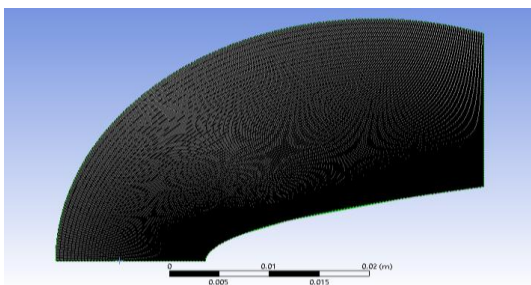


Fig. 8. mesh of 0.5 conical blunt nose profile

After meshing these files are saved and opened in fluent for the solving purpose.

TABLE IV. INPUT DATA (VISCOUS FLOW)

Solver type	Density based, Axisymmetric
Models	Energy (on), Spalart-Allmarms
Materials	Ideal gas, viscosity=Sutherland
Cell zone conditions	Operating pressure = 0
Boundary conditions (Farfield)	Pressure farfield, P=101325, M=2, T=300 Specification-intensity and hydraulic diameter (5, 20)
Boundary conditions (outlet)	Pressure outlet, P=0.1, T=300 Specification=from neighbouring cell
Reference values	Farfield, Area=0.000183093, L=27.9
Solution methods	Flow=first order
Solution controls	Courant number=0.01
Monitors	Edit, criteria change to 1e-6
Monitors	Create, drag
Monitors	Surface monitors, mass flow rate
Solution initialization	Standard, farfield, initialize
Calculation activities	Auto save=500
Run calculation	Iterations=1000, calculate

**V.RESULTS AND DISCUSSION**

Two main computational studies were performed during the course of this study; inviscid flow and the viscous flow over blunt nose profiles of various fineness ratio configurations at different mach numbers. In this chapter, the results from these computational studies will be discussed. The figure.9 and 10 shows static pressure contours of blunt nose profile for mach number 2.

**A. Inviscid flow results**

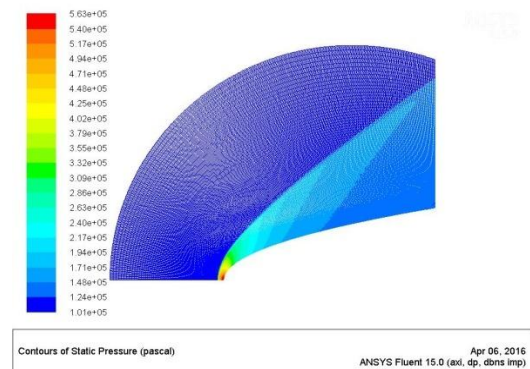


Fig. 9. Static pressure contours of blunt nose profile n = 0.5 for M = 2

B. Viscous flow results

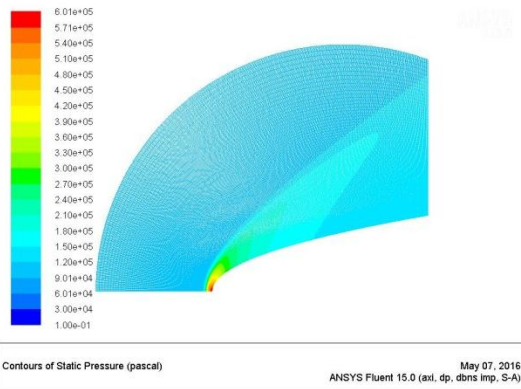


Fig. 10. Static pressure contours of blunt nose profile  $n = 0.5$  for  $M = 2$

TABLE VI. CD VALUES FOR VARIOUS FINENESS RATIOS AND MACH NUMBERS

Mach-2 Inviscid flow	
Fineness ratio	Coefficient of drag
0.5	0.392
0.667	0.215
0.8	0.153

Mach-2 Viscous flow	
Fineness ratio	Coefficient of drag
0.5	0.452
0.667	0.258
0.8	0.19

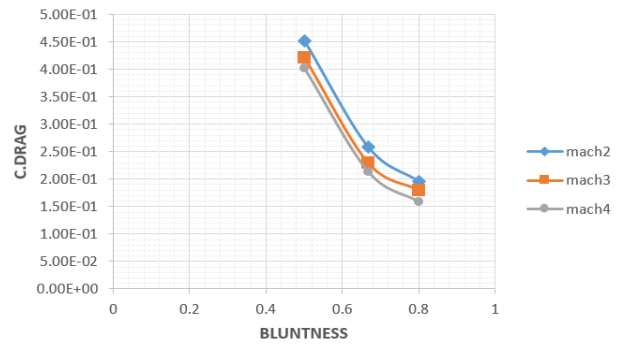
  

Mach-3 Viscous flow	
Fineness ratio	Coefficient of drag
0.5	0.421
0.667	0.229
0.8	0.179

Mach-4 Viscous flow	
Fineness ratio	Coefficient of drag
0.5	0.401
0.667	0.213
0.8	0.159

This investigation showed the above mentioned results. Over all drag coefficient variation over these profiles at different mach numbers is shown in the following plot.1



Plot. 1. Graph showing the drag coefficient variation vs. blunt nose profiles at different mach numbers

VI. CONCLUSION

By increasing the fineness ratio of the nose, it is possible to reduce the overall drag of the projectile. However, increasing the fineness ratio without proper study could possibly result in a higher drag coefficient. Increasing the fineness ratio in fact increases the skin friction drag, while it doesn't contribute much as seen with its small  $C_D$  values compared to the total  $C_D$  but if the fineness ratio is increased beyond the values of the graph it may become more significant as the graph clearly shows an increasing trend.

Also it can be noted that the wave drag is the largest contributor especially at low Mach number and low fineness ratio due to more energy losses. While the base drag is only affected by the Mach number, however as it enters the supersonic speed range the base drag decreases as such it is less of a concern. From this study, a projectile designer aiming to reduce drag should focus more on the wave drag component as it is the largest contributor and care should be taken not to increase the fineness ratio without proper consideration as he may end up increasing drag instead.

From the present investigation we performed on the blunt nosed profiles of fineness ratios  $n = 0.5$ ,  $n = 0.667$ ,  $n = 0.8$ , at various mach numbers, we found that as fineness ratio increases the drag force effect decreases simultaneously. So from this we conclude that as blunt nose with fineness ratio increases from  $n = 0.5$  to  $n = 0.8$  the drag force effect decreases so  $n = 0.8$  turned out to be the best profile at supersonic speeds with minimum effect on drag force due to its bluntness from this investigation.

For further study, it is recommended that Computational Fluid Dynamics (CFD) be used as an additional verification tool due to its current advancement and ease of use in providing and displaying graphics to help understand the airflow around the nose. CFD also allows multiple configurations to be tested initially without resorting to expensive wind tunnel testing.

## REFERENCES

- [1] "The Descriptive Geometry of Nose Cones". The Descriptive Geometry Of Nose Cones- Word document by Gary A. Crowell Sr.
- [2] "Nose cones equations". Nose Cones excel sheet by Kemal Payza. <http://www.info-central.org/?article=125>. Retrieved October 23, 2009.
- [3] Mason, W. H. and Lee, J., "On Optimal Supersonic/Hypersonic Bodies," AIAA Paper 90-3072, 1990.
- [4] Mahdi, A. and Al-Atabi, M. (2008) Effect of Body Shape on the Aerodynamics of Projectiles at Supersonic Speeds. Journal of Engineering Science and Technology (JESTEC), 3 (3), 278-292.
- [5] Mccoy, R. (1981). "MC DRAG"- A Computer Program for Estimating the Drag Coefficients of Projectiles. [report]
- [6] Maryland: US Army Armament Research and Development Command.